Supplementary Material for "Characterizing Superradiant Phase of the Quantum Rabi Model"

Yun-Tong Yang[1,2] and Hong-Gang Luo[1,2,3]

[1] *School of Physical Science and Technology, Lanzhou University, Lanzhou 730000, China*
[2] *Lanzhou Center for Theoretical Physics and Key Laboratory of Theoretical Physics of Gansu Province, Lanzhou University, Lanzhou 730000, China*
[3] *Beijing Computational Science Research Center, Beijing 100084, China*

A. The Born-Oppenheimer approximation

To obtain Eq. (7) in the text, we made the Born-Oppenheimer approximation where the coupling between these two branches $\phi_\pm$ is neglected. In the case of no using the Born-Oppenheimer approximation, Eq. (7) of the text should read

$$\sum_{\pm}(H_0+H_\sigma)\phi_\pm(\xi)\psi_\pm^E(\xi)=\sum_{\pm}E\phi_\pm(\xi)\psi_\pm^E(\xi) \tag{1}$$

Multiplying by $\phi_\pm^*$, Eq. (8) in the main text should read

$$\langle\phi_\pm|H_0|\phi_\mp\rangle\psi_\mp^E(\xi)+(H_{0,\pm}+\epsilon_\pm)\psi_\pm^E(\xi)=E_\pm\psi_\pm^E(\xi), \tag{2}$$

where $\langle\phi_\pm|H_0|\phi_\mp\rangle=-\frac{1}{2}\langle\phi_\pm|\frac{\partial^2}{\partial\xi^2}|\phi_\mp\rangle\neq 0$. In the first diagonalization, the Hamiltonian is divided into negative branch $(H_0+\epsilon_-)$ and positive one $(H_0+\epsilon_+)$. ϕ_- is the wavefunction corresponding to negative branch and ϕ_+ corresponding to positive one. ϕ_- and ϕ_+ could couple each other through the first term in Eq. (2).

Under the Born-Oppenheimer approximation, we provide whole energy spectrum which contains both the negative and positive branches, as shown in Fig. 1(a). The parameter $\Delta=3$ is taken. The orange lines denote the first 6 energy levels of negative branch and the purple lines denote the first 4 energy levels of positive branch. The energy levels of these two branches are independent. The negative one always decreases with increasing the coupling strength, and the positive one always rises. As a result, the higher energy levels of negative branch and the lower energy levels of positive one become intersected each other. Then, we give the first 8 energy levels obtained by exact diagonalization, as shown by circle in Fig. 1(b), which exhibits that the high-energy levels with different parity could intersect for certain Δ for the energy levels we considered. Moreover, those energy levels with the same parity are avoided level-crossing. This avoided crossing is absent in our scheme because of the Born-Oppenheimer approximation we adopted. Fig. 1(c) is the replot of Fig. 1(a) and Fig. 1(b) in order to compare them directly. One can see that the negative branch corresponds to the descending of energy spectrum of ED and the positive branch corresponds to the rising ones. Therefore, the Born-Oppenheimer approximation in our scheme only influences the results near the crossing points of these two branches with the same parity.

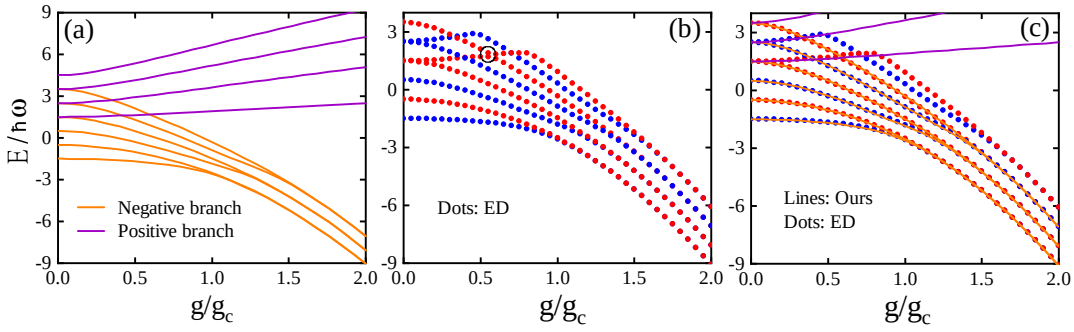

FIG. 1. The energy levels calculated by our method (a) and exact diagonalization (b) for $\Delta=3$ to show the crossings between the high- and low-energy branches. (a) The first 6 energy levels of negative branch (orange lines) and the first 4 energy levels of positive branch (purple lines). (b) The first 8 energy levels obtained by ED. (c) Replots of (a) and (b) in order to compare them in a direct way.

B. The accuracy and convergence rate of our method

To evaluate the convergence and accuracy of our method, we compare each energy level obtained from numerical ED (the truncation is taken $N_{trun} = 500$) with our calculated results by using the formula $\delta E = E_{ED} - E_{ours}$. A crude criterion of whether the system converges is whether δE is zero. Fig. 2 shows δE of the ground state and the other 9 low-lying excited states as functions of the coupling strengths with $\Delta = 10$. For the first 5 energy levels, Fig. 2(a)-(e) show that the system converges in the entire coupling regime up to $g/g_c = 2$ when the truncated basis is $N_{trun} = 30$. For higher energy levels, from the fifth excited state to the ninth excited state, the system converges when we extend the truncated basis up to $N_{trun} = 50$, as shown in Fig. 2(f)-(j).

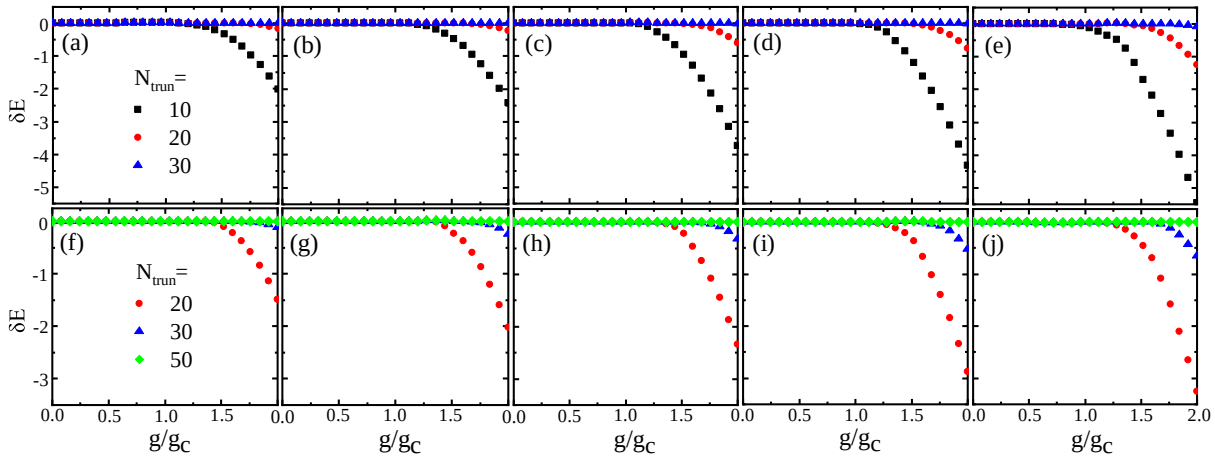

FIG. 2. The difference between ED and our method of each energy level from the ground state (a) to the other 9 excited states (b-j) as functions of the coupling strengths scaled by $g_c = \sqrt{1 + \sqrt{1 + \frac{\Delta^2}{16}}}$.

To evaluate the convergence rate of our method, we compute the ground state energy separately by our method and ED for increasing cutoff. The parameter $\Delta = 10$ is taken. Fig. 3(a) is the energy level of the ground state calculated by our method and Fig. 3(b) is the results of ED. The black, purple, green and blue lines denote different truncations of Fock basis. The red dashed line denote the energy level of the ground state obtained by ED, where the truncation is choosen $N_{trun} = 500$. Fig. 4 indicates that our method and numerical exact diagonalization converge at similar rate in the QRM. The difference between our method and ED is the dimension of matrix to be diagonalized: $N \times N$ for our method but $2N \times 2N$ for ED.

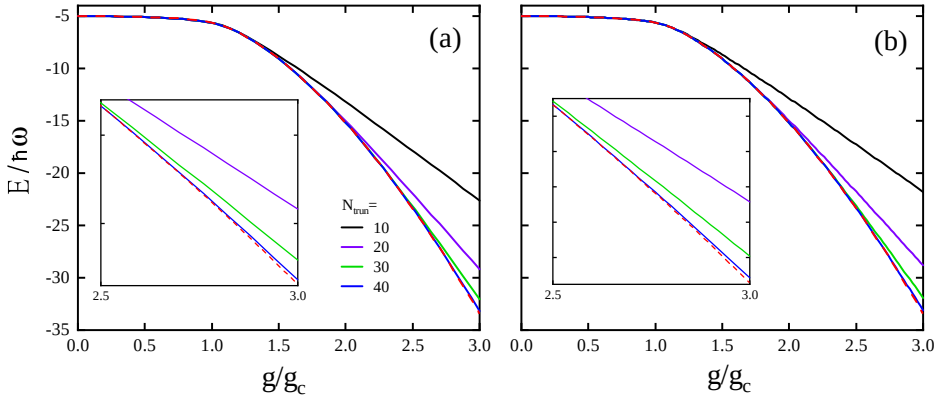

FIG. 3. The ground state energy for different truncations of Fock basis computed by our method (a) and exact diagonalization (b). The black, purple, green and blue lines denote the different truncations, $N_{trun} = 10, 20, 30$ and 40. The red dashed line denote result of ED as benchmark, where the truncation is $N_{trun} = 500$.

C. The fitting parameters of the photon population

We calculate the photon population and the results exhibit some characteristic behaviors, as shown in Fig. 3 and Fig. 4 in the text. In order to check how the photons populate, we borrow three typical level statistical distributions in random matrix theory

$$P_P(s) = e^{-s}, \tag{3}$$

$$P_{GUE}(s) = \frac{32}{\pi^2} s^2 e^{-\frac{4s^2}{\pi}}, \tag{4}$$

$$P_{GOE}(s) = \frac{\pi}{2} s e^{-\frac{\pi s^2}{4}}, \tag{5}$$

which correspond to the Poissonian statistics, the statistics of GUE and GOE. The variable s denotes the energy intervals of adjacent levels in the original definition. Here we replace s by Fock basis n. And we make an overall enlargement by multiplying the parameter b, and replace n with $a(n+c)$ for the GUE and GOE distributions. The specific formulas we used are as follows

$$P_P(n) = be^{-an}, \tag{6}$$

$$P_{GUE}(n) = b\frac{32}{\pi^2}(a(n+c))^2 e^{-\frac{4(a(n+c))^2}{\pi}}, \tag{7}$$

$$P_{GOE}(n) = b\frac{\pi}{2}(a(n+c)) e^{-\frac{\pi(a(n+c))^2}{4}}. \tag{8}$$

The values of fitting parameters a, b and c are listed in Table I.

Fock basis	Even	Odd	Even	Odd	Even	Odd	Even	Odd
FIG. 3	(a2)		(b2)		(c2)		(d2)	
a	0.358	0.372	0.550	0.369	0.565	0.345	0.586	0.321
b	0.441	0.168	0.585	0.088	0.651	0.042	0.670	0.027
FIG. 3	(a3)		(b3)		(c3)		(d3)	
a	0.166	0.166	0.140	0.140	0.119	0.119	0.101	0.101
b	0.209	0.137	0.188	0.104	0.162	0.074	0.139	0.060
c	0.458	0.218	0	-0.746	-3.429	-3.827	-6.426	-6.900
FIG. 4	(a)		(b)		(c)		(d)	
a	0.140	0.140	0.140	0.140	0.200	0.200	0.200	0.200
b	0.188	0.104	0.100	0.195	0.150	0.087	0.090	0.146
c	0	-0.746	-0.600	-0.396	-7.668	-7.822	-7.759	-7.686

TABLE I. The fitting parameters of the Poissonian-like statistics, the statistics of GUE-like and GOE-like in Fig. 3 and Fig. 4 of the main text.